Protein Science (1993), *2*, 1648-1663. Cambridge University Press. Printed in the USA.
Copyright © 1993 The Protein Society

In vitro aging of calmodulin generates isoaspartate at multiple Asn-Gly and Asp-Gly sites in calcium-binding domains II, III, and IV

STEVEN M. POTTER,[1] WILLIAM J. HENZEL,[2] AND DANA W. ASWAD[3]

[1] Department of Psychobiology, University of California, Irvine, California 92717
[2] Department of Protein Chemistry, Genentech, Inc., South San Francisco, California 94080
[3] School of Biological Sciences, University of California, Irvine, California 92717

(RECEIVED April 15, 1993; ACCEPTED June 29, 1993)

Abstract

We have determined the major sites responsible for isoaspartate formation during in vitro aging of bovine brain calmodulin under mild conditions. Protein L-isoaspartyl methyltransferase (EC 2.1.1.77) was used to quantify isoaspartate by the transfer of methyl-^{3}H from *S*-adenosyl-L-[methyl-^{3}H]methionine to the isoaspartyl (α-carboxyl) side chain. More than 1.2 mol of methyl-acceptor sites per mol of calmodulin accumulated during a 2-week incubation without calcium at pH 7.4, 37 °C. Analysis of proteolytic peptides of aged calmodulin revealed that >95% of the methylation capacity is restricted to residues in the four calcium-binding domains, which are predicted to be highly flexible in the absence of calcium. We estimate that domains III, IV, and II accumulated 0.72, 0.60, and 0.13 mol of isoaspartate per mol of calmodulin, respectively. The Asn-97-Gly-98 sequence (domain III) is the greatest contributor to isoaspartate formation. Other major sites of isoaspartate formation are Asp-131-Gly-132 and Asp-133-Gly-134 in domain IV, and Asn-60-Gly-61 in domain II. Significant isoaspartate formation was also localized to Asp-20, Asp-22, and/or Asp-24 in domain I, to Asp-56 and/or Asp-58 in domain II, and to Asp-93 and/or Asp-95 in domain III. All of these residues are calcium ligands in the highly conserved EF-hand calcium-binding motif. Thus, other EF-hand proteins may also be subject to isoaspartate formation at these ligands. The results support the idea that isoaspartate formation in structured proteins is strongly influenced by both the C-flanking residue and by local flexibility.

Keywords: β-aspartate; calcium-binding site; deamidation; EF-hand; flexibility; isoaspartate; protein aging; protein damage; protein-L-isoaspartyl methyltransferase

Isoaspartate (β-carboxyl-linked aspartate) arises spontaneously in proteins and peptides, under physiological conditions of pH and temperature, from deamidation of asparaginyl residues or isomerization of aspartyl residues, by way of a cyclic imide intermediate (Bornstein & Balian, 1977; Johnson et al., 1989b; Stephenson & Clarke, 1989). Protein L-isoaspartyl methyltransferase (PIMT, EC 2.1.1.77), an enzyme found in a wide variety of organisms (O'Connor & Clarke, 1985; Johnson et al., 1991; Li & Clarke, 1992), specifically methylates L-isoaspartyl residues in peptides and proteins, forming labile α-carboxyl methyl esters. The presence of isoaspartate, in which the former side chain is now part of the peptide backbone, can functionally impair peptides and proteins (Gráf et al., 1973; Kanaya & Uchida, 1986; Johnson et al., 1987a; Hallahan et al., 1992). Prolonged methylation by PIMT in vitro has been shown to convert isoaspartyl peptides to the aspartyl form (Johnson et al., 1987b; McFadden & Clarke, 1987; Galletti et al., 1988a) and to partially restore functionality of deamidated CaM (Johnson et al., 1987a). Thus, it is likely that PIMT has evolved to aid in the repair and/or degradation of cellular proteins that have undergone isoaspartate formation.

PIMT has proven to be a useful tool for detecting isoaspartate in peptides and proteins. When the radiolabeled methyl donor [methyl-^{3}H]AdoMet is used in the PIMT-catalyzed reaction, methylated isoaspartate can be quantified in substrates by separating labeled substrates from reactants chromatographically (Johnson & Aswad, 1991) or by monitoring the production of radioactive methanol

Reprint requests to: Dana W. Aswad, School of Biological Sciences, University of California, Irvine, California 92717.

Abbreviations: [methyl-^{3}H]AdoMet, *S*-adenosyl-L-[methyl-^{3}H]methionine; CaM, calmodulin; EGTA, ethyleneglycol-bis-(β-aminoethyl ether) *N*,*N*,*N*′,*N*′-tetraacetic acid; PAGE, polyacrylamide gel electrophoresis; PIMT, protein L-isoaspartyl methyltransferase; PMSF, phenylmethylsulfonyl fluoride; PTH, phenylthiohydantoin; RP-HPLC, reversed-phase high-performance liquid chromatography; SDS, sodium dodecyl sulfate; TFA, trifluoroacetic acid.

from the breakdown of the labile methyl esters upon treatment with mild base (Murray & Clarke, 1984). Concern about the stability and purity of injectable recombinant proteins has led to the use of PIMT in studies of isoaspartate formation during in vitro aging of recombinant human growth hormone (Johnson et al., 1989b) and recombinant tissue plasminogen activator (Paranandi & Aswad, submitted).

The multifunctional calcium-binding protein, calmodulin (see Kinemage 1), has been shown to be a good substrate for PIMT after in vitro aging at pH 7.4, 37 °C (Johnson et al., 1987a, 1989a). CaM is carboxyl-methylated in situ in frog oocytes (Desrosiers et al., 1990), in cultured pituitary cells (Vincent & Siegel, 1987), and in human erythrocytes (Runte et al., 1982; Brunauer & Clarke, 1986), albeit to a very small extent. Asn-Gly sequences are notorious for their propensity toward deamidation, both in peptides and in proteins (reviewed in Wright, 1991). In model peptides of various sequences, the deamidation of Asn residues results in an isoaspartate to Asp ratio of about 3:1 (Bornstein & Balian, 1977; Meinwald et al., 1986; Geiger & Clarke, 1987). CaM contains two Asn-Gly sequences, one in each of the second and third of its four calcium-binding domains. Having observed a nearly stoichiometric relationship between methyl-accepting capacity and ammonia loss following pH 7.4 incubations of CaM, we proposed that one or both of these Asn-Gly sequences were major sites of isoaspartate formation (Johnson et al., 1989a). Ota and Clarke (1989b) have reported that CaM aged in a calcium-free solution for 13 days at pH 7.4, 37 °C, contains isoaspartate at Asp-2-Gln-3 and at Asp-78-Thr-79 and/or Asp-80-Ser-81, and at unspecified locations in or near calcium-binding domains II, III, and IV. The relative contributions of these sites to overall isoaspartate content is difficult to assess from their study because methylation and subsequent analysis were carried out using conditions under which approximately 98% of the potential methylation sites were not characterized (Johnson & Aswad, 1991).

In the present study, we have used a different analytical strategy that has allowed us to account for the location of at least 90% of the isoaspartate formed in CaM during in vitro aging. By localizing the major isoaspartate sites to specific residues, we have significantly expanded the database of sequences in structured proteins that are prone to degradation under mild conditions. The growing list of such sites has important implications for the predictability of damage sites based on amino acid sequence.

Results

The methyl-accepting capacity of native and aged CaM: Effects of trypsinization

CaM purified from bovine cerebral cortex (as described in the Materials and methods) was aged in vitro for 2 weeks at pH 7.4, 37 °C, in the presence of 1 mM EGTA. Control CaM, henceforth referred to as native, was kept at −70 °C in the same buffer during this period. As a first step in localizing aging-induced isoaspartate formation, aged and native CaM were digested with trypsin. Others have observed significant increases in PIMT-catalyzed methyl-accepting capacity as an artifact of proteolytic digestion (Galletti et al., 1988a,b; Artigues et al., 1990). To show that the majority of the isoaspartate we detected in aged CaM arose during in vitro aging and not during the tryptic digestion, we determined the overall methyl-accepting capacities of whole native and aged CaM and of their tryptic digests. Table 1 shows that trypsinization resulted in minor increases in the methyl-accepting capacity of CaM. Because the absolute increase in methyl-accepting capacity for the aged CaM (0.07 mol/mol) was greater than that of the native CaM (0.02 mol/mol), it is likely that the observed increases result mostly from the unmasking of isoaspartate sites that were inaccessible to PIMT in the intact proteins and not from isomerization during the trypsinization. If the trypsinization had caused significant isoaspartate formation, we would expect an equal or greater increase in the methylation of native CaM, compared to aged CaM, because many of the labile sites in aged CaM would have already isomerized during the in vitro aging.

Accurate assessment of isoaspartate by enzymatic methylation occurs over a relatively narrow range of experimental conditions. We have attempted to carry out methylation reactions under optimal conditions of pH, temperature, AdoMet concentration, and time, and to use detection methods that do not rely on the assumption that labile methyl esters will remain intact during the reaction (Johnson & Aswad, 1991). PIMT has an unusually low turnover number (Johnson & Aswad, 1993), so it is important that sufficient enzyme is present to allow complete methylation of the substrate. We tested the methyl-accepting capacity of CaM trypsin digests using varying

Table 1. *Effect of trypsin digestion on the methyl-accepting capacity of native and aged calmodulin (CaM)*[a]

Sample	Methyl incorporation (mol CH_3/mol CaM)
Native CaM – whole	0.012 ± 0.002
Native CaM – trypsin digest	0.034 ± 0.006
Aged CaM – whole	0.76 ± 0.06
Aged CaM – trypsin digest	0.83 ± 0.02

[a] Samples of native and 2-week-aged CaM were digested using trypsin as described in the Materials and methods. Whole and trypsin-digested samples of both native and aged CaM were methylated in triplicate for 40 min in standard reactions containing 2 μM protein L-isoaspartyl methyltransferase (PIMT) and 5 μM intact CaM or CaM digest. Methyl incorporation was assayed by the methanol diffusion method. Values shown are means ± SD.

amounts of PIMT. As shown in Figure 1, the methylation stoichiometry for the digest of aged CaM was approx. 1.2 mol/mol at the highest enzyme concentration used (5 μM). The break in the curve at ~1 μM PIMT suggests that both high-affinity and low-affinity sites are present. The digest of native CaM was methylated to a maximum of 0.05 mol/mol at 3 μM PIMT.

Identification of the major methyl-accepting tryptic peptides in CaM digests

Tryptic peptides from native and aged CaM were separated by RP-HPLC and identified by acid hydrolysis and amino acid composition analysis as described in the Materials and methods. Peaks with compositions corresponding to all of the expected CaM tryptic fragments (Watterson et al., 1980) were observed, as indicated in Figure 2A. The native and aged CaM digests were also chromatographed, under identical conditions, after having been methylated by PIMT using [methyl-^{3}H]AdoMet. Fractions were collected, and radioactivity was determined by liquid scintillation counting.

At the scale used in Figure 2C,D, the methylated native CaM digest showed a small peak at 32 min, while the aged CaM digest showed large peaks of methyl-^{3}H incorporation at 32, 41, 49–51, and 34 min. These are labeled 1–4, respectively, in order of decreasing peak area. These four sites account for 77% of the total radioactivity recovered, with the remainder in small peaks across the run. The radiochromatograms were virtually identical whether the methylation reactions were carried out in the presence of 5 or 14 μM PIMT, indicating that the digest was methylated to the maximum extent possible (data not shown). Integration of the peaks of the radiochromatogram of the native CaM digest gave the same order of peak areas as the aged CaM digest for the four largest methyl acceptors, although at a much lower level of methylation. Except for the peak at 32 min, this is not evident in Figure 2D because of the scale used.

Sites 1–4 correspond in retention time to unmethylated fragments 91–106 (T1), 127–145/148 (T2), 38–71/74/75/77 (T3), and 14–30 (T4), respectively (Fig. 2). However, because the presence of extra methyl groups affects peptide retention times, it was necessary to verify this correspondence. To this end, individual peptides corresponding to each identified peak (those labeled in Fig. 2A, which comprise the entire CaM sequence) were collected from the chromatography of an unmethylated aged CaM digest,

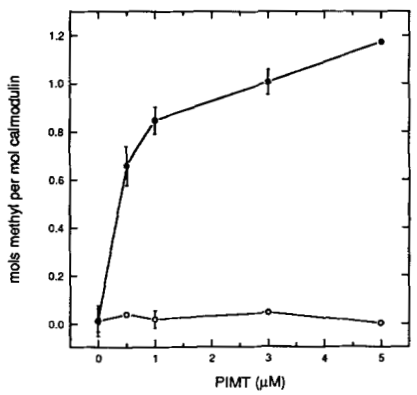

Fig. 1. Methyl incorporation into trypsinized CaM as a function of PIMT concentration. A trypsin digest of 2-week aged CaM (closed circles) or native CaM (open circles) was methylated as described in the Materials and methods, at a concentration equivalent to 1 μM whole CaM, with varying concentrations of PIMT, as indicated on the abscissa. Error bars indicate the range of duplicate reactions and are covered by the plot symbols in some cases. Isoaspartyl delta sleep-inducing peptide was used as a stoichiometry control (Johnson & Aswad, 1991).

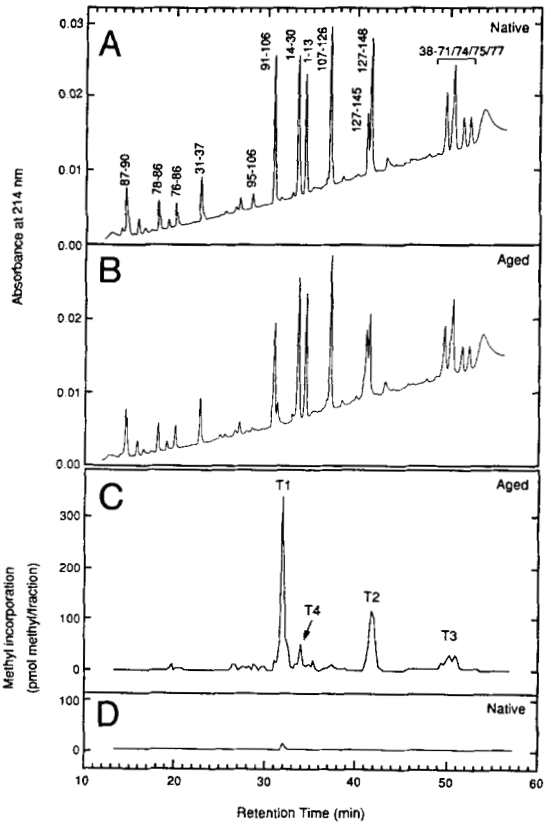

Fig. 2. RP-HPLC of trypsin digests of native and aged CaM, unmethylated and methylated. Ten micrograms of either native (**A**) or aged (**B**) unmethylated CaM were chromatographed on the C-8 reversed-phase column as described in the Materials and methods, using a linear solvent gradient from 0 to 80% B. Peaks were collected, dried under a vacuum, identified by amino acid composition analysis, and subjected to PIMT methylation assays as described in the Materials and methods. Methylated digests of either aged (**C**) or native (**D**) CaM were chromatographed under the same conditions, and radioactivity was quantified by liquid scintillation counting of fractions collected throughout the runs. Counts observed during a blank run (methylated trypsin digest with no CaM present) were subtracted from the radiochromatograms of C and D.

and their methyl-accepting capacities were determined. The peptides with the four largest methyl-accepting capacities were the same as those suggested by the pre-HPLC-methylation experiment, i.e., T1 > T2 > T3 > T4 > all other tryptic peptides.

Detailed analyses of T1, T2, and T3

Analysis of T1

The best methyl-accepting peptide from trypsin digests of native and aged CaM, T1 (91–106), was purified by RP-HPLC using acidic solvents, as in Figure 2. The unresolved peak following the main peak (at 31.2 min in the aged CaM digest) was collected separately. Although it accounted for about 16% of the area of the two peaks (which had the same 214/280-nm absorbance ratios), a methylation assay showed that it had only 4% of the methyl-accepting capacity of the two peaks. Some or all of this methyl-accepting capacity may be due to contamination by material from the larger peak. The possible identity of this overlapping peak will be addressed below. Subsequent T1 experiments were conducted on material from the main 91–106 peak.

RP-HPLC at pH 6 allows separation of deamidated peptides from their Asn-containing progenitors because aspartate and isoaspartate side chains are charged at this pH and Asn side chains are not. One would expect deamidated peptides (Asp/isoaspartate forms) to elute before the native peptides (Asn form) due to this extra charge. Peptide T1 from both native and aged CaM was rechromatographed at pH 6 (Fig. 3), revealing a large early peak at 30 min in the sample from aged CaM, T1a, that accounted for 72% of the total peak area. Peptide T1b (33 min), which coelutes with the main peak in the native chromatogram, accounted for the other 28% of the total peak area. The minor early peak (30 min) from the native CaM sample accounted for only 1.5% of the total peak area.

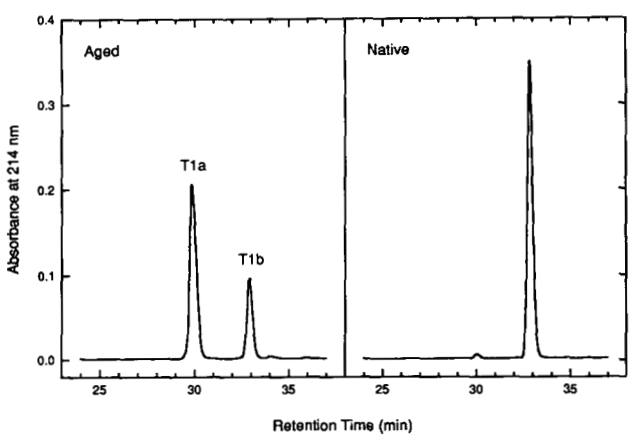

Fig. 3. HPLC of T1 at pH 6. Peptide T1 (91–106) from aged and native CaM was chromatographed on the C-8 column at pH 6 using a linear gradient of 1% B/min after 5 min at 0% B.

Peptide T1a from aged CaM and T1 from native CaM were subjected to mass spectrometry. Deamidation of asparagine residues results in a mass increase of 1.0 amu. Their masses, 1,755.9 amu for T1a and 1,754.9 amu for T1 (the expected mass), were consistent with deamidation at the only asparagine residue in the sequence, Asn-97.

The sequencing of peptides by Edman degradation is blocked at isoaspartate residues (Smyth et al., 1962). Sequencing of T1a, along with T1 as a control for variations in repetitive yields, showed no asparagine and a small amount of aspartate at the seventh cycle, verifying that Asn-97 in T1a was deamidated and that most of it was in the isoaspartate form (Table 2). Much of the aspartate detected at cycle 7 may have resulted from carryover of Asp-95 because there was negligible yield of any amino acids in the eighth cycle of the T1a sequencing.

As mentioned earlier, the deamidation of asparagine-containing sequences in model peptides usually results in the formation of isoaspartate and aspartate in the ratio of about 3:1. The extensive block of T1a sequencing at cycle 7 suggests that the Asp-97 form of the peptide was minimally present. Under the HPLC conditions of Figure 2, it is common for the aspartyl form of a peptide to elute slightly later than the isoaspartyl form (Geiger & Clarke, 1987; Johnson et al., 1987b, 1989b). We presume that the Asp-97 form of T1 accounts for the unresolved peak following the main 91–106 peak of Figure 2B. This interpretation is supported by the finding, mentioned above, that this peak is not a significant methyl-acceptor.

Due to its comigration with the native T1 using pH 6 HPLC, T1b from aged CaM was assumed to be non-deamidated. However, methylation assays showed that this peptide contained a significant amount of isoaspartate: 0.13 mol/mol T1b, or 6% of the total methyl-accepting capacity of T1a and T1b from aged CaM. Apparently, some isoaspartate formation at Asp-93 and/or Asp-95 had occurred. Assuming that isoaspartate formation at one residue is independent of the same at another residue, similar amounts of isoaspartate due to isomeri-

Table 2. *Sequencing yields*[a] *for T1 (91–106) from native CaM and T1a from aged CaM*

Peak	V 91[b]	F 92	D 93	K(D) 94	D 95	G(D) 96	N(D) 97	G 98	Y 99
T1–native	102	119	46	104 (4)	42	123 (13)	63 (11)	74	112
T1a–aged	234	196	73	114 (27)	63	59 (28)	0 (13)	2	–

[a] Yields (pmol of phenylthiohydantoin [PTH] amino acid) are not corrected for carryover into subsequent cycles. Sequencing of T1a was not carried out past the eighth cycle.

[b] Residue number.

zation of Asp-93 and/or Asp-95 would also be expected in T1a, the deamidated form of T1.

We used enzymatic methylation in combination with RP-HPLC at pH 6.0 to investigate the number of isoaspartyl sites in T1a and T1b. The rationale for this approach is based on the fact that stoichiometric methylation converts each isoaspartyl site to a methyl ester and/or a cyclic imide, the latter arising as the immediate breakdown product of the methyl ester (Johnson & Aswad, 1991). For a peptide containing a single site that is a mixture of aspartate and isoaspartate, methylation will lead to a characteristic appearance of two new UV-absorbing species, both with greater retention times than the unmodified peptide (see, for example, Fig. 4 in Johnson et al., 1989b). The later of the two new peaks will be the methyl ester (which will also carry the radiolabel if [methyl-^{3}H]AdoMet is used as the methyl donor). The imide will typically precede the methyl ester and will not carry the label. For a peptide containing two sites, each with a mixture of aspartate and isoaspartate, the pattern of new peaks generated is considerably more complex because either site can exist (after complete methylation of the isoaspartyl fraction) in any of three states: aspartate, cyclic imide, or methyl ester. The possible combinations of peptides generated in such an analysis and their expected relative retention times are summarized in Table 3.

Peptides T1a and T1b were methylated using PIMT and [methyl-^{3}H]AdoMet under conditions that should provide stoichiometric methylation of isoaspartate residues. The results of pH 6 HPLC of the labeled samples and scintillation counting are shown in Figure 4. For peptide T1a, both the UV trace (Fig. 4A) and the radiolabel profile (Fig. 4C) are consistent with the presence of two isoaspartyl sites. The early peak at 10.5 min, which corresponds to the elution position of unmethylated T1a, probably contains Asp at residues 93, 95, and 97. It is reasonable to assume that the middle group of peaks (14–16.5 min) consists of the expected singly methylated peptides and the corresponding cyclic imides, while the late group (18.5–20.5 min) consists of the doubly methylated peptide and the related cyclic imide forms. As predicted by Table 3, the latest-eluting peak (19.8 min) has twice the specific activity (radioactivity per UV area) of either the 15.8-min peak or the 19.2-min peak. After methylation, 6.4% (by UV peak area) of T1a from aged CaM has the same retention time as the unmethylated T1a, 76% elutes in the middle group, and 17% elutes in the late group. If the late group is from the di-isoaspartyl peptide, then it contributes 0.34 mol isoaspartate per mol of T1a (17% × 2), for a total of 1.10 mol (0.76 + 0.34) isoaspartate per mol T1a from both sites.

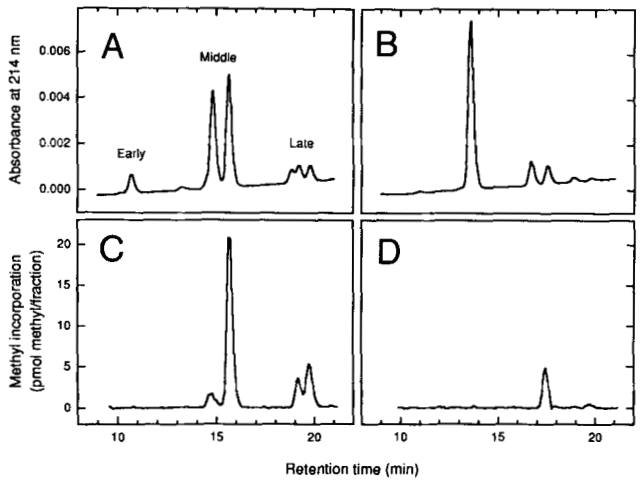

Fig. 4. HPLC of methylated T1 from aged CaM, at pH 6. Approximately 250 pmol of either T1a (**A** and **C**) or T1b (**B** and **D**) from aged CaM were methylated with PIMT and ^{3}H-AdoMet and chromatographed at pH 6.0 on the C-8 column using a linear gradient from 20 to 40% B. Fractions were collected and radioactivity was quantified by liquid scintillation counting (plotted in C and D). A no-substrate blank reaction was also chromatographed, and the background counts were subtracted from the radiochromatograms of C and D.

Table 3. *Expected properties of methylation products for a peptide containing two potential isoaspartyl residues*[a]

Relative retention[b]	Charge	Methyl-^{3}H	Residue 1	Residue 2
Early	−2	0	Asp	Asp
Middle−1	−1	0	Asp	Imide
Middle−1	−1	0	Imide	Asp
Middle−2	−1	1	Asp	Methyl ester
Middle−2	−1	1	Methyl ester	Asp
Late−1	0	0	Imide	Imide
Late−2	0	1	Imide	Methyl ester
Late−2	0	1	Methyl ester	Imide
Late−3	0	2	Methyl ester	Methyl ester

[a] It is assumed that (1) the original peptide contained a mixture of aspartate and isoaspartate at two different sites, and (2) all isoaspartate has been completely converted to methyl ester.

[b] For RP-HPLC at pH 6. The three retention groups (early, middle, and late) are based on charge. Within each of these groups, it is assumed that the net contribution to hydrophobicity (later retention) follows the order, methyl ester > imide > Asp.

Methylation of T1b (Fig. 4B,D) resulted in two new peaks at 16.7 and 17.5 min in the UV trace of Figure 4B. These represent the imide and the methyl ester, respectively, because only the latter of the two was radiolabeled. This pattern indicates the presence of a single isoaspartyl site that must have come from either Asp-93 or Asp-95 because Asn-97 is intact in T1b. The UV peaks at 16.7 and 17.5 min in Figure 4B account for 20% of the total T1b detected.

Assuming that isoaspartate formation at Asp-93/95 is independent of isoaspartate formation at Asn-97, the proportion of isoaspartate at Asp-93/95 should be equal in both T1a and T1b, or 0.2 mol/mol (20%). Thus, we estimated the contribution of isoaspartate in T1a from

Asn-97 to be 0.9 mol/mol T1 (1.1 − 0.2). Assuming there is no isoaspartate at residue 97 of T1b or in the overlapping peak (31.2 min) following the major 91–106 peak from aged CaM (Fig. 2B), then there would be 0.55 mol of isoaspartate at residue 97 per mol of 91–106 from aged CaM ([0.9 mol/mol T1] × [0.72 mol T1a/mol T1] × [0.84 mol major 91–106 peak/total mol 91–106]). The 0.2 mol of isoaspartate derived from Asp-93 or Asp-95 becomes 0.17 mol/mol total 91–106 from aged CaM ([0.2 mol/mol major 91–106 peak] × [0.84 mol major 91–106 peak/total mol 91–106]). The isoaspartate present in the 31.2-min peak overlapping the main T1 peak (Fig. 2) would increase these values slightly, as would the isoaspartate content of the minor 95–106 peptide (28.2 min in Fig. 2), an alternative tryptic cleavage product that has approx. 6% the UV peak area (at 280 nm) of the 91–106 peaks. In sum, the 91–106 sequence contains *at least* 0.72 mol isoaspartate per mol of aged CaM (0.55 for Asn-97 + 0.17 mol/mol for Asp-93 or Asp-95).

The area of the T1 peak in the radiochromatogram of the trypsin digest of native CaM (at 32 min in Fig. 2D) is approx. 3% of the area of the corresponding peak from the aged CaM digest. Thus, only about 0.02 mol/mol of the 0.72 mol/mol of isoaspartate observed in T1 from aged CaM was not a direct consequence of in vitro aging. A detailed analysis of the specific residues containing isoaspartate in native CaM was not undertaken due to the small proportion of isoaspartate in peptides derived from native CaM.

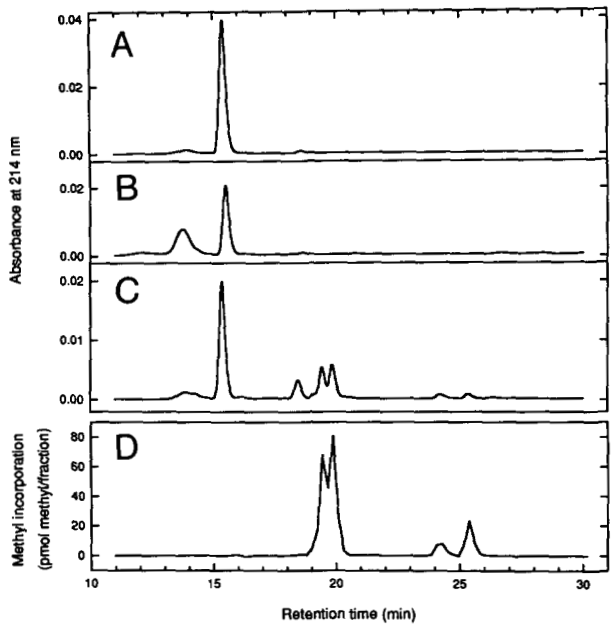

Fig. 5. HPLC of T2C3 at pH 6. Unmethylated T2C3 (127–138) from either native (**A**) or aged (**B**) CaM was chromatographed on the C-8 column at pH 6 using a linear gradient from 0 to 25% B after 5 min at 0% B. Methylated T2C3 from aged CaM was chromatographed under the same conditions (**C**), and radioactivity was quantified by liquid scintillation counting of fractions (**D**). The two small, overlapping peaks near 14 min in C do not have the same A214/A280 ratio as T2C3 and thus are probably unrelated contaminants.

Analysis of T2

Peptide T2 consisted of a mixture of the sequences 127–145 and 127–148, which were not well separated by RP-HPLC (Fig. 2). Therefore, this mixture was further digested with chymotrypsin to produce several shorter peptides that were separated easily by RP-HPLC and identified by amino acid composition analysis (not shown). Two methyl-accepting peptides were produced, from alternative cleavage at Tyr-138 or Phe-141. We used the more abundant of the two for further analysis, the 127–138 peptide (T2C3). Both peptides contain all four of the T2 candidate sites for isoaspartate formation: Asp-129, Asp-131, Asp-133, and Asn-137.

Peptide T2C3 from native or aged CaM was methylated and subjected to pH 6 HPLC. In Figure 5A and B, chromatograms of the unmethylated peptides are shown. Methylated T2C3 from aged CaM (Fig. 5C,D) exhibited a pattern consistent with the presence of isoaspartate at two distinct residues (Table 3). Methylation resulted in a large reduction in the 13.8-min peak, and the appearance of two groups of peaks at 18–20.5 and 23.8–26 min. The radiochromatogram of methylated T2C3 from native CaM (not shown) showed only a small doublet at 19–20 min, representing less than 5% of the area of all of the peaks from methylated T2C3 from aged CaM.

To provide a better separation of the unmethylated forms of T2C3, this sample was chromatographed using TFA/acetonitrile solvents and a shallow gradient, revealing a number of peaks (Fig. 6). The four labeled peaks had a 214/280-nm absorbance ratio of 17. These were sequenced and subjected to mass spectrometry. Peaks at 19.1 and 20.8 min had anomalous absorbance ratios, leading to the conclusion that they were unrelated contaminants.

The sequencing of peak A was completely blocked at Asp-131 (Table 4). Peaks B and C were blocked at Asp-133 and Asp-131, respectively. No blockage of sequencing was detected in any peptide at Asp-129, nor at Asn-137 in the peptides that were not blocked at earlier residues. Peak D and the 127–138 peak derived from native CaM both yielded the expected sequence. Mass spectrometry showed no evidence of deamidation in any of the T2C3 samples, ruling out Asn-137 as an isoaspartate site. These results, along with relative peak size and migration on RP-HPLC, suggest that in vitro aging causes isoaspartate formation at Asp-131 (peak C) and Asp-133 (peak B) at roughly similar rates, and that peak A is the di-isoaspartate form. The UV peak areas of Figure 6 were integrated at two wavelengths (214 and 280 nm) to allow subtraction of contaminant peaks, in order to quantify isoaspartate in T2C3. When the isoaspartate present in the native peptide (about 0.04 mol/mol) is subtracted, we find that

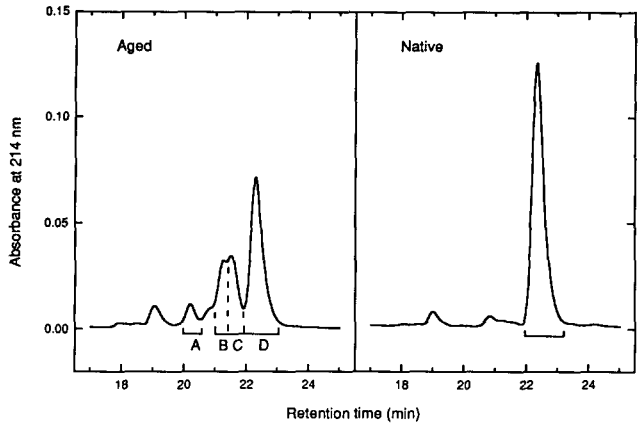

Fig. 6. Acidic HPLC of T2C3. Unmethylated T2C3 from aged or native CaM was chromatographed on the C-8 column using the trifluoroacetic acid (TFA)/acetonitrile solvents described in the Materials and methods. The gradient used was 0–20% B in 5 min after 5 min at 0% B, then from 20 to 27% B in 14 min. The bracketed peaks were further analyzed by sequencing and mass spectrometry (see text and Table 5). The peaks at 19.1 and 20.8 min in both chromatograms had A214/A280 ratios different from that of T2C3. Taken to be unrelated contaminants, these were not further analyzed.

aging results in approximately 0.26 mol isoaspartate at Asp-133 and 0.34 mol isoaspartate at Asp-131, per mol of aged CaM, with 8% of the molecules containing isoaspartate at both residues. Thus, a total of approx. 0.60 mol/mol (0.26 + 0.34) isoaspartate in T2 result from in vitro aging.

Analysis of T3

The third best methyl-accepting tryptic fragment, T3, is the longest, with three asparagine residues and four aspartate residues that could form isoaspartate during in vitro aging. To help eliminate some of these potential sites, the two most abundant T3 peptides (38–71 and 38–74) were digested with endoproteinase Glu-C. Several peptides were purified from the digest by RP-HPLC (Fig. 7) and identified by amino acid composition analysis. Only the 55–67 peptide (35.5–38 min) from aged CaM was a significant methyl-acceptor, with 98% of the methyl-accepting capacity of all five subfragments. This rules out Asn-42, Asp-50, and Asn-53 as sites of significant isoaspartate formation. The remaining candidate sites in the 55–67 peptide are Asp-56, Asp-58, Asn-60, and Asp-64.

In an attempt to characterize aged-modified forms of CaM 55–67, this peptide was rechromatographed by RP-HPLC at pH 6.0, using a shallow gradient of increasing acetonitrile. The aged peptide contained four variants that were either not present or present in much lower amounts in the native peptide (Fig. 8). Three of these variants (peaks A, B, and C) eluted close to each other and well ahead of the native peptide. The fourth variant (D′) appears as a small leading shoulder (62 min) on peak D. The early elution of peaks A, B, and C suggested they were deamidated. This was confirmed by mass spectrometry (Table 5). In contrast, peak D had the mass expected for the native peptide. Because Asn-60 is the only candidate for deamidation, we concluded that A, B, and C are all deamidated at this site.

Deamidation of a single Asn-60 should give rise to a maximum of two early eluting variants (aspartyl and isoaspartyl forms), with one of the two serving as a methyl acceptor. The appearance of three (rather than two) early eluting forms together with the appearance of D′ indicate that at least one other source of heterogeneity is induced during aging. An obvious candidate for this added heterogeneity is isomerization at one of the three aspartyl residues in the 55–67 sequence. Assuming isomerization at this aspartyl site is independent of deamidation of Asn-60, one would expect a total of six forms in the aged 55–67 peptide (two alternatives at the Asp site [α-Asp or β-Asp] × three alternatives at Asn-60 [Asn, α-Asp, or β-Asp]). The pattern of peaks seen in the left panel of Figure 8 is consistent with this hypothesis. Given that β-Asp peptides often elute slightly earlier than their α-Asp counterparts, we would expect peak A to be the di-isoaspartyl peptide, peak B to be a mixture of mono-isoaspartyl peptides, and peak C to be the di-aspartyl form. Peak D′ should be the mono-isoaspartyl form that is not deamidated.

Table 4. *Sequencing yields[a] of T2C3 (127–138) peaks from Figure 6*

Peak	E 127	A 128	D 129	I 130	D 131	G 132	D 133	G 134	Q 135	V 136	N 137	Y 138
Native	148	134	127	137	112	86	102	83	80	134	61	47
Aged – A	13	8.1	7.6	6.5	0	0	–	–	–	–	–	–
Aged – B	83	100	63	77	53	45	0	–	–	–	–	–
Aged – C	51	55	37	47	9	9	0	–	–	–	–	–
Aged – D	83	75	64	45	57	27	40	21	21	23	24	24

[a] Yields (pmol of PTH amino acid) are not corrected for carryover. Dashes indicate values that were not determined.

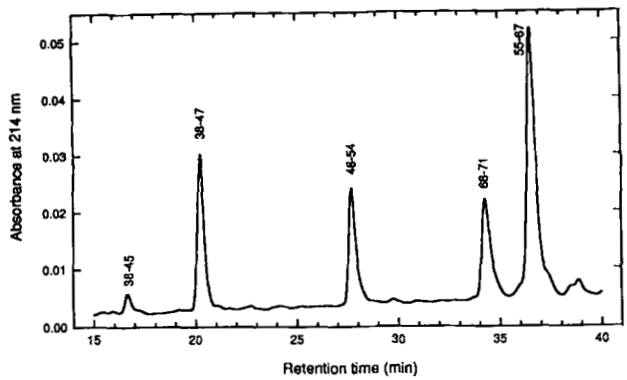

Fig. 7. HPLC of Glu-C digest of T3 (38–71). Peptide T3 from native and aged CaM was digested with endoproteinase Glu-C as described in the Materials and methods and chromatographed on the C-8 column using the TFA/acetonitrile solvents and a linear gradient from 0 to 40% B. The chromatogram of a digest of 38–71 from aged CaM is shown. A digest of 38–74 presented an identical profile, except for the presence of the 68–74 subfragment. Peaks were collected and identified by amino acid composition analysis and assayed for methyl-accepting capacity, as described in the Materials and methods. Only the 55–67 peptide from aged CaM was found to be a significant methyl-acceptor.

Table 5. *Masses and methylation capacities of fragment 55–67 from aged CaM*

Peak[a]	Mass	Methyl incorporation	
		pmol[b]	pmol/unit area[c]
Aged – A	1,350.5	163	1.90
Aged – B	1,350.5	567	1.00
Aged – C	1,350.5	135	0.38
Aged – D	1,349.5	283	0.047

[a] Peaks are labeled as in Figure 8.
[b] Picomoles calculated for the whole peak, based on methyl incorporation into equal-sized aliquots of peaks dried and redissolved in equal volumes.
[c] Picomoles/unit area were normalized so that the value for peak B is one.

To test the above predictions, we assayed the methyl-accepting capacities of peaks A, B, C, and D (including D′) (Table 5). As expected, peak A had twice the methylation capacity found in peak B. The methylation capacity in D + D′ was about the same as that expected if D′ alone were the sole source of isoaspartate in D + D′. The results for peak C are complicated by the fact that this peak, as collected for methylation assays, was heavily contaminated with peak B material. (Using the shape of the native 55–67 peak in Fig. 8 as a model of peak asymmetry, we estimated graphically that 40% of peak C was overlapping peak B material.) Correcting for this contamination indicated that, as expected, C alone is not a significant methyl-acceptor. As a further test of the "two sites" hypothesis, we attempted to sequence peaks A, B, C, and D by Edman degradation. This hypothesis predicts that: peak A would be completely blocked at position 56, 58, or 60; peak B would be completely blocked at position 60 (if the second site is at Asp-54 or Asp-58) or at least partially blocked at position 60 (if the second site is at Asp-64); peak C would yield Asp at position 60 but otherwise give a normal sequence. The sequencing results are shown in Table 6. No sequence data were obtained for peak A (not even a Val in cycle 1), probably due to the small amounts of material recovered. Peak B was completely blocked at position 60. Peak C gave a normal sequence except for the presence of Asp, instead of Asn, at position 60. Peak D gave a completely normal sequence.

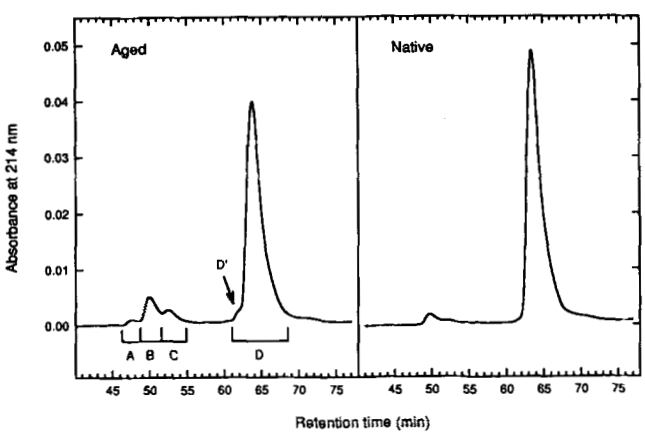

Fig. 8. HPLC of CaM 55–67 at pH 6. The unmethylated 55–67 peptide from aged and native CaM was chromatographed at pH 6 using the C-18 column and a linear gradient from 0 to 25% B in 100 min after 5 min at 0% B. Labeled peaks were collected and assayed for their methyl-accepting capacity (Table 5).

Taken together, the HPLC profile of the aged 55–67 peptide at pH 6, the methylation stoichiometries, and the sequencing results indicate that T3 contains two distinct isoaspartyl sites, one arising from deamidation of Asn-60, the other arising from isomerization at Asp-56, Asp-58, or, less likely, Asp-64. To calculate the overall contribution of site T3 to the isoaspartate content of aged CaM, we used peak areas from Figure 8 to determine the percent contribution of peaks A, B, C, and D + D′ to the aged 55–67 peptide. We then multiplied these percentages by the stoichiometries for each peak (Table 5) and determined that T3 makes an overall contribution of 0.16 mol of isoaspartate per mol of CaM. Assuming that the two sites within T3 form isoaspartate independently of each other, the stoichiometry of peak D leads to the conclusion that the Asp-56, Asp-58, or Asp-64 contributes 0.05 mol of isoaspartate per mol of CaM. Thus, the contribution by Asn-60 is 0.11 (0.16 − 0.05) mol of isoaspartate per mol of CaM. The profile of the native 55–67 peptide in Figure 8 indicates that approx. 25% of peak B did not arise during our in vitro aging. Assuming that this peak

Table 6. *Sequencing yields[a] for Glu-C fragment of T3 (55–67) from native and aged CaM*

Peak	V 55	D 56	A 57	D 58	G 59	N(D) 60	G 61	T 62	I 63	D 64	F 65
Native	31	12	28	8.1	17	12	14	7.2	14	4.4	11
Aged–B	56	30	39	26	31	0	–	–	–	–	–
Aged–C	12	3.4	16	3.3	11	0.0 (2.0)	9.8	3.2	7.9	1.1	6.0
Aged–D	36	17	12	14	11	6.4 (2.6)	9.2	1.8	20	7.9	13

[a] Yields (pmol of PTH amino acid) are not corrected for carryover.

represents mostly the isoaspartyl product of Asn-60 deamidation, we estimate conservatively that the age-dependent contribution of Asn-60 is approx. 0.08 mol of isoaspartate per mol of CaM. These contributions are summarized in Table 7.

Influence of aging on the conformational response to calcium

Because the sites of isoaspartate formation that we have detected all lie within calcium-binding domains, in vitro aging would be expected to result in altered calcium binding. It has been shown that in vitro aging or base treatment results in a number of CaM forms resolvable by nondenaturing PAGE (Johnson et al., 1987a; Desrosiers et al., 1990). Here, we expand on these techniques in a way that emphasizes calcium-dependent changes in gel mobility. Whole native and aged CaM were separated by two-dimensional nondenaturing PAGE in the presence of 2 mM EGTA in the first dimension and in the presence of 1.5 mM calcium chloride in the second dimension. Figure 9 shows that aging causes a marked conversion of the native form into a number of forms with aberrant migration on this gel system, presumably altered in their calcium binding and/or conformational responses to calcium.

Table 7. *Estimated contributions of individual residues to the isoaspartate content of aged CaM*

Tryptic fragment	Calcium-binding domain	Isoaspartate contribution[a] Residue	Per residue	Per fragment
T1	III	Asp-93/95	0.17	0.72
		Asn-97	0.55	
T2	IV	Asp-131	0.34	0.60
		Asp-133	0.26	
T3	II	Asp-56/58/64	0.05	0.13
		Asn-60	0.08	

[a] In moles isoaspartate per mole aged CaM. The small contribution not associated with in vitro aging has been subtracted away. The values reported here depend, in part, on the assumption that isoaspartyl residues were stoichiometrically methylated by PIMT; thus, they may represent lower limits of isoaspartate content.

Discussion

Locations of isoaspartate sites

Using PIMT to label isoaspartate-containing fragments of in vitro aged CaM and a combination of HPLC, protein sequence analysis, and mass spectrometry, we have determined which residues are most likely to form isoaspartate in CaM under the aging conditions we employed (14 days at pH 7.4, 37 °C, without calcium). The locations

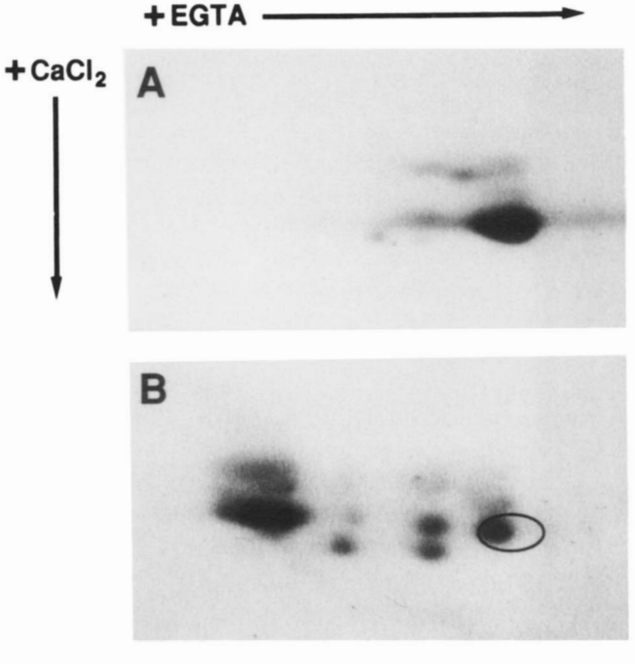

Fig. 9. Two-dimensional (±calcium) nondenaturing polyacrylamide gel electrophoresis (PAGE) of native and aged CaM. Ten micrograms of either native (**A**) or aged (**B**) CaM were subjected to two-dimensional nondenaturing PAGE in the presence of 2 mM EGTA in the first dimension and 1.5 mM calcium chloride in the second dimension, as described in the Materials and methods. Gels were stained with Coomassie R-250. The ellipse in B indicates the corresponding position of the main spot on the gel of native CaM.

of the major isoaspartate sites in aged CaM are denoted with asterisks in Figure 10 (Kinemage 1). Isoaspartate was also localized to one or more of the residues marked with dots, per tryptic fragment, i.e., to at least three of these residues in the whole molecule. The single greatest source of isoaspartate in aged CaM is Asn-97. This is one of two Asn–Gly sequences that were suggested previously as a major source of isoaspartate in aged CaM (Johnson et al., 1985, 1989a). A substantial amount of isoaspartate was localized to Asp sites as well: Asp-131 and Asp-133 contribute 0.34 and 0.26 mol/mol, respectively. Aging-induced isoaspartate formation amounting to at least 0.1 mol/mol was localized to Asp residues at positions 56, 58, and/or 64 in T3, and positions 20, 22, and/or 24 in T4. Candidate sites Asp-20 and Asp-93 are followed by Lys residues, and Asp-64 by a Phe residue. Neither Asp–Lys nor Asp–Phe pairs have been observed to form isoaspartate readily in model peptides, and therefore they may not be significant contributors to the isoaspartate we observed in the corresponding proteolytic fragments. Thus, it seems likely that nearly all of the isoaspartate that formed during aging was at Asn–Gly or Asp–Gly pairs.

An earlier study of CaM deamidation (Johnson et al., 1989a) reported that 2 weeks of aging at pH 7.4, 37 °C, resulted in the loss of 0.75 mol of ammonia per mol of CaM. This is consistent with the data in Table 7, which attribute 0.63 mol of isoaspartate per mol of CaM to deamidation of Asn-97 and Asn-60. Asparagines degrading via the succinimide pathway typically generate 0.70–0.85 mol of isoaspartate per mol of asparagine. The ratio of isoaspartate contributed by Asn-97 plus Asn-60 (Table 7) to ammonia release is 0.84 (0.63/0.75), suggesting that nearly all of the deamidation of CaM under these mild conditions goes through the succinimide pathway. The earlier study estimated the *total* isoaspartate content of 2-week aged CaM at 0.60 mol/mol of CaM, implying that nearly all of the isoaspartate was derived from deamidated asparagine. According to Table 7, however, the total level of isoaspartate is approx. 1.45 mol/mol CaM, with 57% coming from isomerization of aspartic acid. The previous underestimate of total isoaspartate can be attributed to limitations of the methylation assay (see Johnson & Aswad, 1991) used in the earlier study.

All of the major isoaspartate sites in aged CaM lie within calcium-binding loops, as shown in Figure 10 (Kinemage 1). The confirmed isoaspartate sites (marked with asterisks) correspond to the Y and Z ligands of the octahedral calcium complex (Kretsinger, 1987). Candidates for the minor isoaspartate sites that we were unable to localize precisely, marked with dots, are also calcium ligands in this complex. This can explain the observation that calcium inhibits isoaspartate formation in a dose-dependent manner (Johnson et al., 1989a; Ota & Clarke, 1989b).

CaM is a member of a large family of proteins that contain multiple copies of this highly conserved calcium-

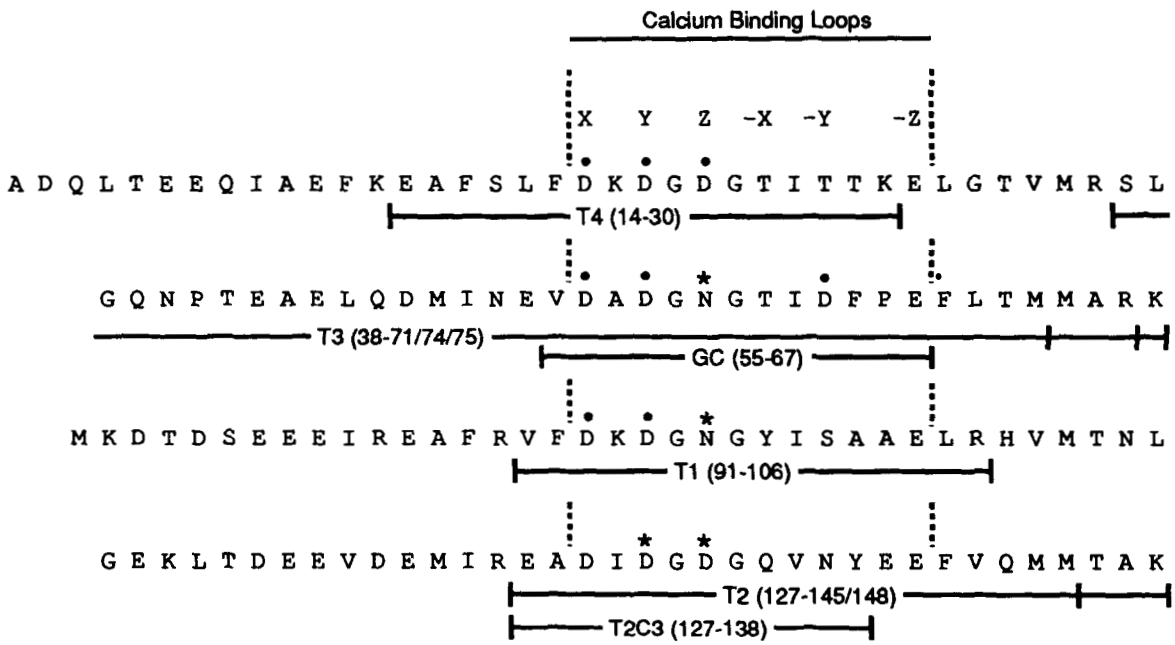

Fig. 10. Bovine brain CaM sequence. Location of major isoaspartate sites. The sequence is presented with the six calcium-binding ligands (labeled X through −Z) of all four calcium-binding domains aligned. The major isoaspartate sites were localized to the proteolytic fragments produced by trypsin (T1–T4), endoproteinase Glu-C (GC), and chymotrypsin (T2C3), as indicated by underlines. Asterisks indicate the major residues shown in this study to form isoaspartate during in vitro aging. Aging also causes isoaspartate formation in at least one of the dotted residues per tryptic fragment in which dotted residues are shown. The atypical cleavage by trypsin after Met-71 and Met-145 has been noted previously (Watterson et al., 1980).

binding motif, known as the EF-hand (reviewed in Persechini et al., 1989). Kretsinger and coworkers have compiled a database of all known EF-hand sequences (Nakayama & Kretsinger, 1993). Out of the 243 known sequences, each with 2–6 EF-hand domains, 227 (93%) contain at least one Asx–Gly in the Y or Z position. More than 60% of all the putative calcium-binding domains in the database have Asx–Gly at the Y or Z positions.

Urea denaturation of recombinant calbindin D_{9k} has been shown to promote isoaspartate formation at Asn-56 (Chazin et al., 1989). Like the two deamidation sites of CaM, this is the Y ligand of the EF-hand domain of calbindin D_{9k}. (The other calcium-binding site of calbindin D_{9k} is not a traditional EF-hand [Brodin et al., 1986].) Because of the conservation of the tertiary structure of the EF-hand motif (Babu et al., 1988) and of its primary sequence, it seems likely that other EF-hand proteins readily form isoaspartate at these calcium ligands in the absence of calcium.

Possible role of local sequence and flexibility in determining sites of isoaspartate formation

The major isoaspartyl sites we detected in aged CaM (asterisks, Fig. 10; Kinemage 1) occur in Asn–Gly or Asp–Gly pairs, and it is likely that the isoaspartate associated with T4 may also occur in one or both of its Asp–Gly pairs. In flexible peptides, formation of isoaspartate at Asn–X or Asp–X bonds occurs most rapidly at neutral pH when X is Gly or Ser (Geiger & Clarke, 1987; Stephenson & Clarke, 1989; Capasso et al., 1991). Although conformational restrictions in structured proteins have the capacity to override simple sequence effects (Clarke, 1987; Kossiakoff, 1988), there is a growing body of examples wherein deamidation and/or isomerization under in vivo or mild in vitro conditions occurs most rapidly at these same sequence pairs. Examples include triosephosphate isomerase (Yuksel & Gracy, 1986), bovine seminal ribonuclease (Di Donato et al., 1986), epidermal growth factor (DiAugustine et al., 1987), trypsin (Kossiakoff, 1988), recombinant human growth hormone (Johnson et al., 1989b), serine hydroxymethyltransferase (Artigues et al., 1990), angiogenin (Hallahan et al., 1992), recombinant tissue plasminogen activator (Paranandi & Aswad, submitted), and now CaM (the present study).

Domains with a high degree of conformational flexibility might permit the formation of isoaspartate at a significantly higher rate than would otherwise occur in a more structured domain (Clarke, 1987; Johnson et al., 1989b). We used the flexibility plot of Ragone et al. (1989) to see if the sites of isoaspartate formation found in CaM arise in regions predicted to have above-average flexibility. This plot is based on the premise that flexibility is enhanced in regions that are rich in residues with small and/or polar side chains. Figure 11A shows that all four of the calcium-binding domains, including all of the major isoaspartate sites, do indeed fall in the regions predicted to have above-average flexibility. Shown in Figure 11B and Kinemage 1 are the regions (marked by dark bars) where α-helices are present in solution, as determined by multidimensional NMR (Ikura et al., 1991). The regions of high predicted flexibility all lie between the helices, including all of the major isoaspartate sites. The Ragone flexibility values for 9 of the 12 candidate isoaspartate sites are above the average flexibility value for all of the Asx residues in CaM. However, the flexibility values of these sites do not correlate well with their relative contributions to the total isoaspartate in aged CaM (compare Table 7 and Fig. 11).

We performed a similar analysis of chain flexibility of CaM using the method of Karplus and Schulz (1985). This method is based on average flexibility ratings for each of the 20 amino acids derived from their temperature factors (*B*-values) in a set of proteins of known X-ray crystal structure. The set did not include CaM. The X-ray crystal structure of CaM *in the presence of calcium* has been determined (Babu et al., 1988). However, the temperature factors would not be expected to apply to the calcium-free form, whose X-ray crystal structure has not been determined. Although it is based on a different approach than the method of Ragone et al., the Karplus and Schulz method produced remarkably similar results. The observed isoaspartate sites are all predicted to lie within flexible domains of the protein (Fig. 11C).

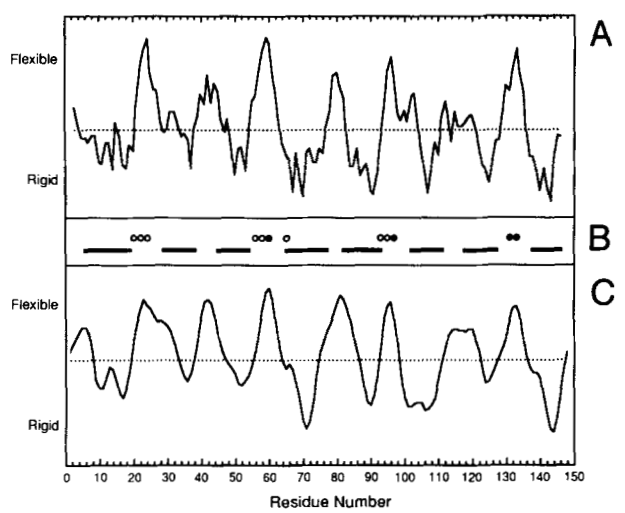

Fig. 11. Flexibility plots of CaM. **A:** Relative side-chain hydrophobicity/volume products are plotted by the method of Ragone et al. (1989), using a five-residue sliding window. Peaks correspond to smaller, more hydrophobic residues **B:** Bars indicate the regions that form α-helices (Ikura et al., 1991). Solid circles correspond to the asterisks of Figure 10, residues in which isoaspartate formation has been confirmed. Open circles correspond to the dots of Figure 10; isoaspartate was present at one or more of these per tryptic fragment T1, T3, and T4. **C:** Flexibility analysis by the method of Karplus and Schulz (1985), based on average X-ray crystallography temperature factors. In A and C, the dotted lines indicate the average value for all residues.

Two-dimensional proton NMR spectroscopy has been used to investigate regional flexibility in calbindin D_{9k} (Skelton et al., 1990; Akke et al., 1991). The calcium-binding domains were found to be highly flexible in the absence of calcium but much less so in its presence. A decrease in flexibility upon calcium binding is consistent with the observation that 10 μM calcium dramatically inhibits isoaspartate formation in calmodulin during in vitro aging (Johnson et al., 1989a).

Ota and Clarke (1989a,b) have reported that Asp-2 and Asp-78 and/or Asp-80 are "major sites" of methylation (and presumably, isoaspartate formation) in "affinity-purified" CaM. In one study (Ota & Clarke, 1989b), in which the CaM was aged in vitro under conditions almost identical to those used here, they also observed methylation associated with proteolytic fragments containing the second, third, and fourth calcium-binding domains, but only in samples that were aged in the absence of calcium. Calcium was proposed to prevent isoaspartate formation by limiting the flexibility of the calcium-binding domains. Assessing the relative contribution of different residues to the methylation they observed is difficult. They methylated CaM with PIMT and radiolabeled AdoMet, then digested it with various proteases, and looked for radioactivity coeluting with proteolytic fragments of native, unmethylated CaM on RP-HPLC. Under the methylation and digestion conditions used, it is likely that the more labile methyl esters were extensively demethylated. Given that demethylation and isoaspartate formation occur via the same cyclic imide intermediate, these are the very sites most likely to form isoaspartate in the first place and would not be detected under the conditions of their analysis. Further, the concentrations of AdoMet and PIMT used were such that sites with a high K_m for PIMT might not have been methylated (Johnson & Aswad, 1991). The presence of charged residues near an isoaspartate residue has been reported to greatly increase the K_m for PIMT in some model peptides (Lowenson & Clarke, 1990). Thus, the isoaspartate sites we observed within the calcium-binding domains, which have nearby charged residues (Fig. 10), may only be well methylated under optimal reaction conditions. Ota and Clarke (1989b) reported a five-fold increase in the methylation of CaM after 13 days incubation at 37 °C and pH 7.4, in the absence of calcium (compared to at least a 63-fold increase in the present study). Moreover, the absolute level of methylation of aged CaM reported by Ota and Clarke (0.015 mol/mol) is less than 2% of the level for intact, aged CaM reported here (Table 1). As shown in Figure 1 and Table 7, the value reported in Table 1 for intact, aged CaM is an underestimate of the total methyl-accepting capacity of aged CaM.

For aged CaM, low levels of methylation are evident in Figure 2C at retention times close to those of peptide 1–14 (35–36 min) and peptide 76–86 (20 min). These are the peptides that contain Asp-2 and Asp-78/80, respectively. Low levels of methylation at these retention times were also observed for native CaM; however, this is not evident in Figure 2D because of the scale used. The low stoichiometry of methyl incorporation observed for these minor sites is consistent with the levels reported by Ota and Clarke (1989a,b). Because they are minor compared with sites T1, T2, and T3, we chose not to characterize them further.

The plus/minus calcium two-dimensional nondenaturing PAGE system revealed that aging resulted in a number of CaM forms that were altered in calcium binding and/or conformational response to calcium (Fig. 9). Because all of the major isoaspartate sites of aged CaM were calcium ligands (Fig. 10), it is likely that the formation of isoaspartate at these sites was responsible for the aberrant gel migration. An altered conformational response to calcium due to isoaspartate formation could be responsible for the aging-induced impairment of CaM's ability to stimulate the calcium/CaM-dependent protein kinase from rat brain (Johnson et al., 1987a). Using CaM that was aged in vitro for 28 days under the same conditions used in this study, Johnson et al. (1987a) observed a PIMT-catalyzed increase from 18 to 68% of the kinase-stimulating activity of native CaM. Because the majority of the isoaspartate in aged CaM originated from aspartate residues (Table 7), the PIMT-catalyzed conversion of isoaspartate to aspartate (Johnson et al., 1987b; McFadden & Clarke, 1987; Galletti et al., 1988a) would restore those sites to their native form.

It is uncertain whether the formation of isoaspartate in CaM in vivo is significant enough to affect its many cellular functions. It is interesting to note that calcium-binding domains III and IV, which contribute most to isoaspartate formation, are also the two with the highest affinity for calcium (Klee et al., 1986). In vivo, CaM is expected to be in the calcium-free state most of the time, due to the extremely low baseline cytosolic calcium concentration (10^{-8}–10^{-7} M; Cheung, 1979). However, the rate of isoaspartate formation in vivo may be less than that observed in vitro because of the possibility for association with other cellular proteins that would limit the flexibility of CaM. Robinson and Robinson (1991) have proposed that amide residues, and specifically, neighboring sequences that encourage deamidation, could serve as "molecular clocks," regulating the functional lifetime of proteins. Not only deamidation but also isoaspartate formation from both asparagine and aspartate residues could be important in regulating protein turnover.

Materials and methods

CaM purification

CaM was purified from bovine cerebral cortex essentially according to the method of Gopalakrishna and Anderson (1982). Modifications or additions to this procedure are

noted below. All steps were conducted at 4 °C except the chromatography, which was conducted at room temperature and took approx. 3 h. About 160 g of tissue was homogenized in two volumes of 50 mM Tris-acetate, pH 7.5, 1.0 mM EDTA, 1.5 mM β-mercaptoethanol, 0.5 mM PMSF, using an Ultra-Turrax homogenizer with an 18K shaft. The homogenate was centrifuged for 45 min at 13,000 rpm in a Sorvall GSA rotor. The supernatant fraction was saved and the pellet rehomogenized as above. The second homogenate was centrifuged as above, and the supernatant fraction was combined with the first supernatant fraction. This cytosolic fraction was brought to 55% saturation in ammonium sulfate (360 g/L) in order to precipitate many unwanted proteins. Dibasic sodium phosphate, 1.0 M, was added as necessary to keep the pH of the solution above 6.5. The solution was centrifuged for 30 min at 12,000 rpm in the GSA rotor and the pellet discarded. The supernatant fraction was then brought to the isoelectric point of CaM, pH 4.2, with cold 50% (v/v) sulfuric acid. After 1 h without stirring, the solution was centrifuged for 10 min at 9,000 rpm in the GSA rotor. The supernatant fraction was discarded, and the pellet was dissolved in a minimum volume of 0.1 M Tris-HCl, pH 8.4. This solution was dialyzed against high-calcium buffer (50 mM Tris-HCl, pH 7.5, 1.0 mM calcium chloride, 1.5-mM β-mercaptoethanol). The dialysate was loaded onto a 15-mL column of phenyl-Sepharose (Sigma) that had been equilibrated with high-calcium buffer; 100 mL of high-calcium buffer was passed through the column. A flow rate of 1–2 mL/min was used in this and subsequent steps. Next, 100 mL of high-salt buffer (50 mM Tris-HCl, pH 7.5, 0.1 mM calcium chloride, 0.5 M sodium chloride, 1.5 mM β-mercaptoethanol) was passed through the column. CaM was eluted from the column with calcium-free buffer (50 mM Tris-HCl, pH 7.5, 1 mM EGTA, 1.5 mM β-mercaptoethanol). CaM from several chromatographic runs was combined and concentrated by isoelectric precipitation as above. It was dialyzed against a solution of 5% (v/v) glycerol in water and stored at −70 °C. The final yield was about 100 mg/kg of cortex. Protein concentrations were determined by the method of Lowry et al. (1951) after precipitating proteins with 7% trichloroacetic acid using bovine serum albumin (Sigma) as the standard.

In vitro aging

Solutions containing 130 μM CaM in aging buffer (50 mM K-HEPES, pH 7.4, 1 mM EGTA, and 0.05% [w/v] sodium azide) were incubated in 1-mL glass Reacti-Vials (Pierce) at 37 °C for 2 weeks. Control (native) CaM in the same buffer was kept at −70 °C during this time. Both the native and the aged CaM were subsequently stored at −14 °C.

Two-dimensional electrophoresis (± calcium)

The following is an adaptation of the nondenaturing discontinuous polyacrylamide gel system described previously (Johnson et al., 1987a). The stacking and main gels had the same composition for both dimensions; the samples were loaded in the presence of EGTA for the first dimension and in the presence of calcium for the second dimension, as described below. SDS and disulfide reducing agents were omitted from all solutions (CaM has no Cys residues). The main gel was 15% (w/v) acrylamide (37.5:1, w/w, acrylamide to *N,N'*-methylene-bisacrylamide ratio), 373 mM Tris-HCl, pH 8.8, 6.6 mM TEMED, and 0.1% (w/v) ammonium persulfate. The stacking gel was 4.8% acrylamide, 126 mM Tris-HCl, pH 6.8, 13 mM TEMED, and 0.1% (w/v) ammonium persulfate. Gels were cast and run using the Bio-Rad Mini-Protean two-dimensional system. Capillaries for the first dimension (75 × 1 mm i.d.) were coated (on the inside only) with Sigmacote siliconizing fluid, to allow easy extrusion of the gels. The capillaries were completely filled with main gel solution. After this was polymerized, the capillaries were removed from the casting tube, and 1 cm of gel was extruded from the top and cut off. The capillaries were then inverted and filled with stacking gel solution. This procedure is necessary to produce a flat interface between the main and stacking gels. Protein samples (5–10 μg per gel) for the first dimension were mixed with 3× concentrated sample buffer and water to produce final concentrations of 2 mM EGTA, 126 mM Tris-HCl, pH 7.0, 10% (v/v) glycerol, 0.003% (w/w) bromophenol blue. Running buffer for both dimensions was 25 mM Tris base, 192 mM glycine, pH 8.8. The first dimension was run at 100 V, until the bromophenol blue dye had left the gels. Tube gels were extruded and placed over slab gels (1 × 82-mm-wide × 47-mm-high main gel, 10-mm-high stacking gel) and overlayed with 100 μL of 3× sample buffer in which the EGTA was replaced with 1.5 mM calcium chloride. After 15 min equilibration in sample buffer, the second dimension was run at 200 V, until the bromophenol blue had left the gels. Gels were stained with Coomassie R-250 and dried under a vacuum.

Proteolytic digests

Trypsin

CaM, either native or aged, at 2 mg/mL in aging buffer was digested by adding trypsin (Sigma) to a final concentration of 3 μM and incubating at 37 °C for 2 h. Then an equal amount of trypsin was added, and the incubation was continued for an additional 2 h. Solutions that would subsequently undergo enzymatic methylation were stopped by adding PMSF to a final concentration of 4 mM and incubating an additional 10 min at 37 °C before storing at

−14 °C. Otherwise solutions were stopped by adding 1/10 volume of 88% phosphoric acid and stored at −14 °C.

Glu-C

Endoproteinase Glu-C (*Staphylococcus aureus* V8 protease, Miles Scientific) was dissolved in water with 5% glycerol (v/v) to a final concentration of 1 mg/mL (1.8 μL/unit) and stored at −14 °C. Peptides were dissolved in 50 mM sodium phosphate, pH 7.8, to a final concentration of 15–20 μM. Enzyme was added to a final concentration of 3 μM and solutions were incubated for 4 h at 37 °C. Reactions were stopped by freezing at −14 °C.

Chymotrypsin

Peptides were dissolved to 2–3 mg/mL in 50 mM sodium phosphate, 1 mM EGTA, 0.05% sodium azide, pH 7.2, and digested with 0.5 mg/mL α-chymotrypsin (Sigma) at 37 °C for 12 h. Reactions were stopped by freezing at −14 °C.

Acid hydrolysis and amino acid composition analysis

Peptides (100–500 pmol) were eluted from HPLC columns into 12 × 75-mm Kimax glass tubes that had been baked previously at 500 °C for 4 h to pyrolyze any contaminating amino acids or proteins. The HPLC solvent was evaporated in the Speed Vac. To each tube was added 200 μL of 6 N HCl (Baker) containing 0.1% (v/v) thioglycolic acid (Sigma). An appropriate amount of norleucine (Sigma) was also added as an internal standard. The tubes were sealed under a vacuum with a torch and heated in a Multi-Blok heater (Lab-Line Instruments) at 115 °C for 24 h. (Occasionally *S*-methylcysteine [Sigma] was used instead of norleucine as an internal standard because norleucine partially coelutes with leucine during subsequent HPLC. It was found that *S*-methylcysteine is partially degraded during the acid hydrolysis, so in cases where it was used as an internal standard, it was added after the hydrolysis step.) After hydrolysis, the contents of the tubes were transferred to microfuge tubes using pasteur pipets. (The microfuge tubes and the pipets had been soaked previously in 6 N HCl for several hours to remove any contaminating amino acids.) The acid was evaporated in the Speed Vac, followed by two additions and evaporations of 200 μL Milli-Q-purified water, to remove all residual HCl.

The dried hydrolysates were dissolved in 80 μL of 0.4 M sodium borate, pH 9.5, 2% SDS. The solutions were derivatized by reaction at room temperature for exactly 1 min with 20 μL of *o*-phthaldialdehyde reagent (Jones, 1986). Reactions were stopped by lowering the pH with 100 μL of 0.2 M monobasic sodium phosphate. Half the volume of the stopped solutions was immediately injected onto a reversed-phase column (Rainin Dynamax C-18 Microsorb Short-One). Solvent A was 0.1 M sodium acetate, pH 6.85. Solvent B was acetonitrile (Burdick & Jackson, UV grade). A Gilson model 121 fluorometer was used, with excitation at 305–395 nm and detection at 430–470 nm. Solvent was pumped at 1.2 mL/min (nominal pressure: 2.8 kpsi) according to the following gradient: 6–15% B in 15 min, 15–22% B in 0.5 min, 22–25% B in 12.5 min, 25–50% B in 4 min, 50–75% B in 0.5 min, hold at 75% B for 2 min to wash column, and return to 6% B in 2 min. Peak areas were integrated with a Gilson Data Master and compared to those of a standard amino acid mixture (Pierce standard "H") to which norleucine or *S*-methylcysteine had been added. Blanks consisting of HPLC solvent and an internal standard carried through all steps of the hydrolysis process were subtracted from peptide hydrolysates, after correcting for recoveries. These typically contained 0–5 pmol of the most abundant contaminants.

Mass spectrometry

Mass spectra were acquired with a JEOL JMS-HX110HF/HX110HF tandem mass spectrometer utilizing MS-1 only. The instrument was operated at a resolution of 3,000 and an accelerating voltage of 10 kV. Ions were formed by fast atom bombardment with a JEOL FAB gun producing 6-keV Xe atoms. Spectra were acquired at a rate of 6–12 s per scan for a mass range of 1,000–3,000 U.

Protein sequencing

Automated Edman degradation was performed on Applied Biosystems 470A and 477A protein sequencers equipped with a 120A PTH analyzer. Sequence interpretation was performed on a Vax 8650 (Henzel et al., 1987).

Methylation reactions

PIMT (M_r = 24,500) was purified from bovine cerebral cortex as previously described (Henzel et al., 1989). The enzyme transferred between 14 and 20 nmol of methyl groups per min per mg to γ-globulin (Sigma). Methylation reactions were carried out in 62 mM sodium phosphate, 20 mM sodium citrate, 2 mM EDTA at 30 °C for 30 min. They contained 0.2 mM [methyl-^{3}H]AdoMet (200–1,000 dpm/pmol, New England Nuclear). The specific activity of the active diastereomer was verified by the method of Hoffman (1986). Unless otherwise indicated, the reactions contained 2–5 μM enzyme and, at most, 20 μM substrate. Reactions were stopped by freezing at −14 °C, unless a diffusion assay was to be performed (see below). Before methylation, peptides purified by HPLC at pH 6 were desalted by rechromatography using TFA/acetonitrile solvents, followed by evaporation to dryness.

Methanol diffusion assays

Methylation reactions (usually 50 μL per tube) were stopped by adding an equal volume of 0.4 M sodium borate, pH 10.2, 4% SDS (w/v), 2% methanol (v/v). Half of the stopped reaction was applied to filter paper in the cap of a 5-mL shell vial. The vials were filled with 2.5 mL of scintillation fluid (Liquiscint) and heated at 40 °C for at least 1 h. During this incubation, carboxylmethyl esters are hydrolyzed, and the ^{3}H-methanol produced diffuses into the scintillation fluid. The caps were then replaced with empty caps and the vials were counted in a Beckman scintillation counter. The channels ratio method was used to convert between cpm and dpm.

HPLC

Unless otherwise indicated, solvent A was 0.1% (w/v) TFA in water, and solvent B was 0.1% (w/v) TFA in a 1:1 (v/v) water/acetonitrile mixture. For the pH 6.0 runs, solvent A was 10 mM sodium phosphate, pH 6.0, and solvent B was a 1:1 mix of solvent A with acetonitrile. The C-8 reversed-phase column used was a 4.6 × 100-mm Aquapore RP-300 (Brownlee Labs) and the C-18 reversed-phase column used was a 4.6 × 220-mm Spheri-5 RP-18 (Brownlee Labs). Absorbance was monitored at 214 nm with a Spectroflow 757 (Kratos) and/or at 280 nm with a Chiratech UV-106 (Linear). Data were integrated with either an HP3396A integrator (Hewlett Packard) or with the Dynamax HPLC Method Manager (Rainin) on a Macintosh IIcx. Radioactive fractions were mixed with at least two volumes of Liquiscint scintillation cocktail and counted on the LS 7500 (Beckman) liquid scintillation counter. Chromatography of methylated samples was preceded by control runs in which no-substrate-methylation blank reactions were injected. Radioactivity recovered during these control runs was subtracted from corresponding fractions in the experimental runs.

Acknowledgments

We thank Dr. John T. Stults for mass spectrometric analyses. This work was supported by U.S. Public Health Service grants NS-17269 and NS-29421. S.M.P. was supported in part by a U.S. Public Health Service National Research Service Award to the Department of Psychobiology, MH-14599.

References

Akke, M., Forsen, S., & Chazin, W.J. (1991). Molecular basis for cooperativity in Ca^{2+} binding to calbindin D_{9k}: ^{1}H nuclear magnetic resonance studies of (Cd^{2+})1-bovine calbindin D_{9k}. *J. Mol. Biol. 220*, 173–189.

Artigues, A., Birkett, A., & Schirch, V. (1990). Evidence for the in vivo deamidation and isomerization of an asparaginyl residue in cytosolic serine hydroxymethyltransferase. *J. Biol. Chem. 265*, 4853–4858.

Babu, Y.S., Bugg, C.E., & Cook, W.J. (1988). Structure of calmodulin at 2.2 Å resolution. *J. Mol. Biol. 204*, 191–204.

Bornstein, P. & Balian, G. (1977). Cleavage at Asn–Gly bonds with hydroxylamine. *Methods Enzymol. 47*, 132–145.

Brodin, P., Grundstrom, T., Hofmann, T., Drakenberg, T., Thulin, E., & Forsen, S. (1986). Expression of bovine intestinal calcium binding protein from a synthetic gene in *Escherichia coli* and characterization of the product. *Biochemistry 25*, 5371–5377.

Brunauer, L.S. & Clarke, S. (1986). Methylation of calmodulin at carboxylic acid residues in erythrocytes. *Biochem. J. 236*, 811–820.

Capasso, S., Lelio, M., & Zagari, A. (1991). Deamidation via cyclic imide of asparaginyl peptides: Dependence on salts, buffers, and organic solvents. *Peptide Res. 4*, 234–238.

Chazin, W.J., Kordel, J., Thulin, E., Hofmann, T., Drakenberg, T., & Forsen S. (1989). Identification of an isoaspartyl linkage formed upon deamidation of bovine calbindin D_{9k} and structural characterization by 2D ^{1}H NMR. *Biochemistry 28*, 8646–8653.

Cheung, W.Y. (1979). Calmodulin plays a pivotal role in cellular regulation. *Science 207*, 19–27.

Clarke, S. (1987). Propensity for spontaneous succinimide formation from aspartyl and asparaginyl residues in cellular proteins. *Int. J. Peptide Protein Res. 30*, 808–821.

Desrosiers, R.R., Romanik, E.A., & O'Connor, C.M. (1990). Selective carboxyl methylation of structurally altered calmodulins in *Xenopus* oocytes. *J. Biol. Chem. 265*, 21368–21374.

DiAugustine, R.P., Gibson, W.A., Kelly, M., Ferrua, C.M., Tomooka, Y., Brown, C.F., & Walkers, M. (1987). Evidence for isoaspartyl (deaminated) forms of mouse epidermal growth factor. *Anal. Biochem. 165*, 420–429.

Di Donato, A., Galletti, P., & D'Alessio, G. (1986). Selective deamidation and enzymatic methylation of seminal ribonuclease. *Biochemistry 25*, 8361–8368.

Galletti, P., Ciardiello, A., Ingrosso, D., Di Donato, A., & D'Alessio, G. (1988a). Repair of isopeptide bonds by protein carboxyl *O*-methyltransferase: Seminal ribonuclease as a model system. *Biochemistry 27*, 1752–1757.

Galletti, P., Ingrosso, D., Pontoni, G., Oliva, A., & Zappia, V. (1988b). Mechanism of protein carboxyl methyl transfer reactions: Structural requirements of methyl accepting substrates. *Adv. Exp. Med. Biol. 231*, 229–245.

Geiger, T. & Clarke, S. (1987). Deamidation, isomerization, and racemization at asparaginyl and aspartyl residues in peptides. *J. Biol. Chem. 262*, 785–794.

Gopalakrishna, R. & Anderson, W.B. (1982). Ca^{2+}-induced hydrophobic site on calmodulin: Application for purification of calmodulin by phenyl-Sepharose affinity chromatography. *Biochem. Biophys. Res. Commun. 104*, 830–836.

Gráf, L., Hajos, G., Patthy, A., & Cseh, G. (1973). The influence of deamidation on the biological activity of porcine adrenocorticotropic hormone (ACTH). *Horm. Metab. Res. 5*, 142–143.

Hallahan, T.W., Shapiro, R., Strydom, D.J., & Vallee, B.L. (1992). Importance of asparagine-61 and asparagine-109 to the angiogenic activity of human angiogenin. *Biochemistry 31*, 8022–8029.

Henzel, W.J., Rodriguez, H., & Watanabe, C. (1987). Computer analysis of automated Edman degradation and amino acid analysis data. *J. Chromatogr. 404*, 41–52.

Henzel, W.J., Stults, J.T., Hsu, C.-H., & Aswad, D.W. (1989). The primary structure of a protein carboxyl methyltransferase from bovine brain that selectively methylates L-isoaspartyl sites. *J. Biol. Chem. 264*, 15905–15911.

Hoffman, J.L. (1986). Chromatographic analysis of the chiral and covalent instability of *S*-adenosyl-L-methionine. *Biochemistry 25*, 4444–4449.

Ikura, M., Spera, S., Barbato, G., Kay, L.E., Krinks, M., & Bax, A. (1991). Secondary structure and side-chain ^{1}H and ^{13}C resonance assignments of calmodulin in solution by heteronuclear multidimensional NMR spectroscopy. *Biochemistry 30*, 9216–9228.

Johnson, B.A. & Aswad, D.W. (1991). Optimal conditions for the use of protein L-isoaspartyl methyltransferase in assessing the isoaspartate content of peptides and proteins. *Anal. Biochem. 192*, 384–391.

Johnson, B.A. & Aswad, D.W. (1993). Kinetic properties of bovine brain protein L-isoaspartyl methyltransferase determined using a synthetic isoaspartyl peptide substrate. *Neurochem. Res. 18*, 87–94.

Johnson, B.A., Freitag, N.E., & Aswad, D.W. (1985). Protein carboxyl methyltransferase selectively modifies an atypical form of calmodulin. *J. Biol. Chem. 260*, 10913–10916.

Johnson, B.A., Langmack, E.L., & Aswad, D.W. (1987a). Partial repair of deamidation-damaged calmodulin by protein carboxyl meth-

yltransferase. *J. Biol. Chem. 262*, 12283–12287.
Johnson, B.A., Murray, E.D., Clarke, S., Glass, D.B., & Aswad, D.W. (1987b). Protein carboxyl methyltransferase facilitates conversion of atypical L-isoaspartyl peptides to normal L-aspartyl peptides. *J. Biol. Chem. 262*, 5622–5629.
Johnson, B.A., Ngo, S.Q., & Aswad, D.W (1991). Widespread phylogenetic distribution of a protein methyltransferase that modifies L-isoaspartyl residues. *Biochem. Int. 24*, 841–847.
Johnson, B.A., Shirokawa, J.M., & Aswad, D.W. (1989a). Deamidation of calmodulin at neutral and alkaline pH: Quantitative relationships between ammonia loss and the susceptibility of calmodulin to modification by protein carboxyl methyltransferase. *Arch. Biochem. Biophys. 268*, 276–286.
Johnson, B.A., Shirokawa, J.M., Hancock, W.S., Spellman, M.W., Basa, L.J., & Aswad, D.W. (1989b). Formation of isoaspartate at two distinct sites during in vitro aging of human growth hormone. *J. Biol. Chem. 264*, 14262–14271.
Jones, B.N. (1986). Amino acid analysis by *o*-phthaldialdehyde precolumn derivatization and reverse-phase HPLC. In *Methods of Protein Microcharacterization* (Shively, J.E., Ed.), pp. 121–151. Humana Press, Clifton, New Jersey.
Kanaya, S. & Uchida, T. (1986). Comparison of the primary structures of ribonuclease U2 isoforms. *Biochem. J. 240*, 163–170.
Karplus, P.A. & Schulz, G.E. (1985). Prediction of chain flexibility in proteins. *Naturwissenschaften 72*, 212–213.
Klee, C.B., Newton, D.L., Ni, W.-C., & Haiech, J. (1986). Regulation of the calcium signal by calmodulin. *Ciba Found. Symp. 122*, 162–182.
Kossiakoff, A.A. (1988). Tertiary structure is a principal determinant to protein deamidation. *Science 240*, 191–194.
Kretsinger, R.H. (1987). Calcium coordination and the calmodulin fold: Divergent versus convergent evolution. *Cold Spring Harbor Symp. Quant. Biol. 52*, 499–510.
Li, C. & Clarke, S. (1992). Distribution of an L-isoaspartyl protein methyltransferase in eubacteria. *J. Bacteriol. 174*, 355–361.
Lowenson, J. & Clarke, S. (1990). Identification of isoaspartyl-containing sequences in peptides and proteins that are unusually poor substrates for the class II protein carboxyl methyltransferase. *J. Biol. Chem. 265*, 3106–3110.
Lowry, O.H., Rosebrough, N.J., Farr, A.L., & Randall, R.J. (1951). Protein measurement with the Folin phenol reagent. *J. Biol. Chem. 193*, 265–275.
McFadden, P.N. & Clarke, S. (1987). Conversion of isoaspartyl peptides to normal peptides: Implications for the cellular repair of damaged proteins. *Proc. Natl. Acad. Sci. USA 84*, 2595–2599.
Meinwald, Y.C., Stimson, E.R., & Scheraga, H.A. (1986). Deamidation of the asparaginyl-glycyl sequence. *Int. J. Peptide Protein Res. 28*, 79–84.
Murray, E.D. & Clarke, S. (1984). Synthetic peptide substrates for the erythrocyte protein carboxyl methyltransferase. *J. Biol. Chem. 259*, 10722–10732.
Nakayama, S. & Kretsinger, R.H. (1993). Evolution of EF-hand calcium-modulated proteins. III. Exon sequences confirm most dendrograms show significant lack of parallelism. *J. Mol. Evol. 36*, 458–476.
O'Connor, C.M. & Clarke, S. (1985). Specific recognition of altered polypeptides by widely distributed methyltransferases. *Biochem. Biophys. Res. Commun. 132*, 1144–1150.
Ota, I.M. & Clarke, S. (1989a). Enzymatic methylation of L-isoaspartyl residues derived from aspartyl residues in affinity-purified calmodulin. The role of conformational flexibility in spontaneous isoaspartyl formation. *J. Biol. Chem. 264*, 54–60.
Ota, I.M. & Clarke, S. (1989b). Calcium affects the spontaneous degradation of aspartyl/asparaginyl residues in calmodulin. *Biochemistry 28*, 4020–4027.
Persechini, A., Moncrief, N.D., & Kretsinger, R.H. (1989). The EF-hand family of calcium-modulated proteins. *Trends Neurosci. 12*, 462–467.
Ragone, R., Facchiano, A., Facchiano, A.M., & Colonna, G. (1989). Flexibility plot of proteins. *Protein Eng. 2*, 497–504.
Robinson, A.B. & Robinson, L.R. (1991). Distribution of glutamine and asparagine residues and their near neighbors in peptides and proteins. *Proc. Natl. Acad. Sci. USA 88*, 8880–8884.
Runte, L., Jurgensmeier, H.-L., Unger, C., & Soling, H.D. (1982). Calmodulin carboxylmethyl ester formation in intact human red cells and modulation of this reaction by divalent cations in vitro. *FEBS Lett. 147*, 125–130.
Skelton, N.J., Kordel, J., Forsen, S., & Chazin, W.J. (1990). Comparative structural analysis of the calcium free and bound states of the calcium regulatory protein calbindin D_{9k}. *J. Mol. Biol. 213*, 593–598.
Smyth, D.G., Stein, W.H., & Moore, S. (1962). On the sequence of residues 11 to 18 in bovine pancreatic ribonuclease. *J. Biol. Chem. 237*, 1845–1850.
Stephenson, R.C. & Clarke, S. (1989). Succinimide formation from aspartyl and asparaginyl peptides as a model for the spontaneous degradation of proteins. *J. Biol. Chem. 264*, 6164–6170.
Vincent, P.L. & Siegel, F.L. (1987). Carboxymethylation of calmodulin in cultured pituitary cells. *J. Neurochem. 49*, 1613–1622.
Watterson, D.M., Sharief, F., & Vanaman, T.C. (1980). The complete amino acid sequence of the Ca^{2+}-dependent modulator protein (calmodulin) of bovine brain. *J. Biol. Chem. 255*, 962–975.
Wright, H.T. (1991). Nonenzymatic deamidation of asparaginyl and glutaminyl residues in proteins. *Crit. Rev. Biochem. Mol. Biol. 26*, 1–52.
Yuksel, K.U. & Gracy, R.W. (1986). In vitro deamidation of human triosephosphate isomerase. *Arch. Biochem. Biophys. 248*, 452–459.